Mon. Not. R. Astron. Soc. **000**, 000–000 (0000) Printed 19 January 2013 (MN LATEX style file v2.2)

arXiv:1104.0859v1 [astro-ph.HE] 5 Apr 2011

Effects of Stress Evolution Process on the Thermal Stability of Thin Accretion Discs

Da-Bin Lin, Wei-Min Gu*, and Ju-Fu Lu
Department of Physics and Institute of Theoretical Physics and Astrophysics, Xiamen University, Xiamen, Fujian 361005, China

ABSTRACT
The stress evolution process is taken into account in the linear stability analysis of standard thin accretion discs. We find that the growth rate of thermally unstable modes can decrease significantly owing to the stress delay, which may help to understand the quasi-periodic variability of GRS 1915+105. We also discuss possible application of stress evolution to the stability of Shapiro-Lightman-Eardley disc.

Key words: accretion, accretion discs — hydrodynamics — instabilities

1 INTRODUCTION

The standard thin accretion disc (Shakura & Sunyaev 1973) has been extensively applied to a variety of astrophysical systems, such as active galactic nuclei, X-ray binaries, and cataclysmic variable stars. The theory of the standard thin disc, which is based on the α stress prescription, predicts that the disc will suffer both thermal and viscous instability when the pressure is dominated by radiation pressure. However, observations of X-ray binaries show little evidence for such instabilities except for GRS 1915+105 (hereafter GRS 1915). Since the stability is related to the description of stress, the standard α stress prescription was modified in some previous works to assure the disc to be stable no matter whether gas or radiation pressure dominates. For instance, Lightman & Eardley (1974) introduced a so-called β stress prescription, i.e., the stress is proportional to the gas pressure rather than the sum of the gas and radiation pressure. With the β stress, the disc will remain stable even for the case that radiation pressure dominates over gas pressure. Furthermore, some other stress prescriptions were introduced by assuming that the stress is relevant to both the total pressure and the gas pressure (e.g., Kato et al. 2008, p. 108). As pointed out by Gierliński, & Done (2004), however, the β stress would be in conflict with observations as follows. Observations show that the colour temperature correction remains stable for a wide range of luminosity, whereas discs with β stress should have a colour temperature correction that changes from ~ 1.8 to ~ 2.7 as the accretion rate increases. Conversely, the standard α prescription may predict that the correction should remain stable at ~ 1.8 for varying accretion rates. Moreover, some recent simulations (e.g., Hirose et al. 2009) showed that the stress is roughly proportional to the sum of gas and radiation pressure. Thus, the standard α prescription seems to be more acceptable than other prescriptions such as the β stress.

The slim disc model was introduced by Abramowicz et al. (1988), in which it was predicted that the thermal instability of the radiation-pressure-dominated thin disc will trigger a limit cycle behaviour between the thin disc and the slim disc. Such a limit cycle was confirmed by time-dependent numerical calculations (e.g., Szuszkiewicz & Miller 2001; Li et al. 2007). On the other hand, Belloni et al. (1997) applied the limit cycle theory to interpret the observational quasi-periodic variability of GRS 1915. Recently, such limit cycle has also been applied to young radio galaxies (e.g., Czerny et al. 2009; Wu 2009). Comparing the numerical results with the observational ones, however, we can find the following inconsistency between the theory and the observation. The numerical results of Li et al. (2007) showed that the duration of the outburst phase $t_{\rm high}$ is less than 5 percent of the duration of the quiescent phase $t_{\rm low}$, and the luminosity of the outburst phase $L_{\rm high}$ is around two orders of magnitude larger than that of the quiescent phase $L_{\rm low}$; whereas observations of GRS 1915 showed that, $t_{\rm high}$ is comparable to $t_{\rm low}$ and $L_{\rm high}$ is only 3-20 times larger than $L_{\rm low}$ (e.g., Belloni et al. 1997; Wu et al. 2010). Some efforts have been made to improve the theory in order to explain observations either by some artifical viscosity prescription (e.g., Nayakshin et al. 2000) or by additional assumption of the energy exchange between the disc and corona (Janiuk et al. 2002).

In the present paper, we will investigate this issue through another way by taking the stress evolution process into account. Our paper is organized as follows. In Section 2, we describe the basic assumption for the stress evolution process. The time-dependent equations and linear stability analysis are presented in Sections 3 and 4, respectively. Conclusions and discussion are made in Section 5.

---

* E-mail: guwm@xmu.edu.cn

2 MODEL

The stress in MHD accretion discs can be expressed as (e.g., Balbus & Papaloizou 1999)

$$\tau_{r\varphi} = < \rho \delta v_r \delta v_\varphi - \frac{\delta B_r \delta B_\varphi}{4\pi} >_\varphi \ , \tag{1}$$

where $\delta v_r (\delta B_r)$ and $\delta v_\varphi (\delta B_\varphi)$ are the fluctuating components of the velocity (the magnetic field) in r and φ direction, respectively. The angled bracket notation denotes the azimuthal average.

The above formula is a general form and is complicated for calculation. In the study of accretion discs, a more practical formula, i.e., the α stress prescription (Shakura & Sunyaev 1973), is widely adopted:

$$\tau_{r\varphi} = -\alpha p_{\rm tot} \ , \tag{2}$$

where $p_{\rm tot}$ is the total pressure, and α is regarded as a constant less than unity. With the above simple form, the α stress prescription has been extensively applied to the research of accretion discs, even in the disc stability analysis. But in the real system, when the pressure varies, it will take a certain period for the stress to adjust. As mentioned in § 1, the stability is sensitive to the description of stress, thus the stress evolution process may have essential effects on the stability. In this paper, we will modify the standard α stress prescription by taking the stress delay into account.

Generally, the growth rate of the stress should be related to $\tau_{r\varphi}^{\rm exp}$ and $\tau_{r\varphi}$, where $\tau_{r\varphi}^{\rm exp}$ is the expected stress and $\tau_{r\varphi}$ is the current stress. Thus we have the following general function for the evolution of stress:

$$\frac{\partial \tau_{r\varphi}}{\partial t} + v_r \frac{\partial \tau_{r\varphi}}{\partial r} = f(\tau_{r\varphi}^{\rm exp}, \tau_{r\varphi}) \ , \tag{3}$$

where v_r is the radial velocity. In a quasi-stationary state, the function f should match the following conditions:

$$\left\{ \begin{array}{ll} f(\tau_{r\varphi}^{\rm exp}, \tau_{r\varphi}) < 0; & \tau_{r\varphi} > \tau_{r\varphi}^{\rm exp} \\ f(\tau_{r\varphi}^{\rm exp}, \tau_{r\varphi}) = 0; & \tau_{r\varphi} = \tau_{r\varphi}^{\rm exp} \\ f(\tau_{r\varphi}^{\rm exp}, \tau_{r\varphi}) > 0; & \tau_{r\varphi} < \tau_{r\varphi}^{\rm exp} \end{array} \right. . \tag{4}$$

In the present paper, we adopt a simple form as follows:

$$f(\tau_{r\varphi}^{\rm exp}, \tau_{r\varphi}) = \frac{\tau_{r\varphi}^{\rm exp} - \tau_{r\varphi}}{t_{\rm ps}} \ , \tag{5}$$

where $t_{\rm ps}$ is the timescale of stress delay for varying pressure. We further adopt $\tau_{r\varphi}^{\rm exp} = -\alpha p_{\rm tot}$ according to the α prescription, where α is a constant. Combining equations (3) and (5), the evolution equation of the stress tensor is

$$\frac{\partial \tau_{r\varphi}}{\partial t} + v_r \frac{\partial \tau_{r\varphi}}{\partial r} = \frac{-\alpha p_{\rm tot} - \tau_{r\varphi}}{t_{\rm ps}} \ . \tag{6}$$

3 EQUATIONS

We first present the time-dependent equations of accretion discs for stability analysis. We consider an axisymmetric, Keplerian rotating disc ($\Omega = \Omega_{\rm K}$) under cylindrical coordinates (r, φ, z). The basic vertically integrated equations are described as follows (e.g., Kato et al. 2008):

$$\frac{\partial \Sigma}{\partial t} + \frac{1}{r}\frac{\partial}{\partial r}(r \Sigma v_r) = 0 \ , \tag{7}$$

$$\Sigma v_r \frac{1}{r}\frac{\partial}{\partial r}(r^2 \Omega) = \frac{1}{r^2}\frac{\partial}{\partial r}(r^2 T_{r\varphi}) \ , \tag{8}$$

$$\Omega_{\rm K}^2 H^2 = \frac{\Pi}{\Sigma} \ , \tag{9}$$

$$\frac{\partial E}{\partial t} - (E + \Pi)\frac{\partial \ln \Sigma}{\partial t} + \Pi \frac{\partial {\rm ln} H}{\partial t} = Q_{\rm vis}^+ - Q_{\rm adv}^- - Q_{\rm rad}^- \ , \tag{10}$$

$$\Pi = \Pi_{\rm gas} + \Pi_{\rm rad} = \frac{k_{\rm B}}{\mu m_{\rm H}} \Sigma T + \frac{2a}{3} T^4 H \ , \tag{11}$$

where $\Sigma = 2\rho H$ is the surface mass density, $\Pi = 2 p_{\rm tot} H$, $T_{r\varphi} = 2\tau_{r\varphi} H$, and E are the vertically integrated pressure, stress, and internal energy, respectively. T is the temperature, H is the half-thickness of the disc, $k_{\rm B}$ is Boltzmann constant, μ is the mean molecular weight, $m_{\rm H}$ is the hydrogen mass, and a is radiation constant. The quantities $Q_{\rm vis}^+$, $Q_{\rm adv}^-$, and $Q_{\rm rad}^-$ represent the viscous heating, advective cooling, and radiative cooling rates, respectively. The expressions of E, $Q_{\rm vis}^+$, $Q_{\rm adv}^-$, and $Q_{\rm rad}^-$ are the following:

$$E = \left[3(1-\beta) + \frac{\beta}{\gamma - 1} \right] \Pi \ ,$$

$$Q_{\rm vis}^+ = T_{r\varphi}(r\frac{d\Omega}{dr}) \ ,$$

$$Q_{\rm adv}^- = v_r \left[-(E + \Pi)\frac{\partial {\rm ln}\, \Sigma}{\partial r} + \frac{\partial E}{\partial r} + \Pi \frac{\partial {\rm ln}\, H}{\partial r} \right] \ ,$$

$$Q_{\rm rad}^- = \frac{16acT^4}{3\bar{\kappa}\Sigma} \ ,$$

where β is defined as the ratio of the gas pressure to the total pressure, i.e., $\beta \equiv \Pi_{\rm gas}/\Pi$, γ is the ratio of specific heating, and $\bar{\kappa}$ is the opacity.

Since the timescale for establishment of vertical equilibrium is the dynamic timescale, which is much shorter than the thermal timescale, we modify the stress evolution process (Eq. [6]) as

$$\frac{\partial T_{r\varphi}}{\partial t} + v_r \frac{\partial T_{r\varphi}}{\partial r} = \frac{-\alpha \Pi - T_{r\varphi}}{t_{\rm ps}} \ . \tag{12}$$

4 STABILITY ANALYSIS

Now we have the set of six equations, i.e., Eqs. (7)-(12) for linear stability analysis, and the corresponding six physical quantities are Σ, Π, v_r, H, T, and $T_{r\varphi}$. With subscript 0 denoting the quasi-stationary solution, and subscript 1 denoting perturbation quantities, we define the following dimensionless variables:

$$\sigma = \frac{\Sigma_1}{\Sigma_0}, \ \xi = \frac{\Pi_1}{\Pi_0}, \ u = \frac{v_{r,1}}{r\Omega}, \ h = \frac{H_1}{H_0}, \ m = \frac{T_1}{T_0}, \ l = \frac{T_{r\varphi,1}}{-\alpha \Pi_0}.$$

With the assumption that all the perturbation quantities are proportional to $\exp(\omega t - ikr)$, the perturbed equations corresponding to Eqs. (7)-(12) can be written as follows:

$$\frac{\omega}{\Omega}\sigma - ikru = 0 \ , \tag{13}$$

$$\frac{\kappa^2}{2\Omega^2} u = i\alpha kr (\frac{1}{r\Omega})^2 \frac{\Pi_0}{\Sigma_0} l \ , \tag{14}$$

$$2h = \xi - \sigma \ , \tag{15}$$

$$\frac{\omega}{\Omega}[3(1-\beta) + \frac{\beta}{\gamma - 1}]\xi + \frac{\omega}{\Omega}\beta \frac{4 - 3\gamma}{\gamma - 1}\frac{1-\beta}{4-3\beta}(-3\xi + 4\sigma - h)$$
$$- \frac{\omega}{\Omega}(4 - 3\beta + \frac{\beta}{\gamma - 1})\sigma + \frac{\omega}{\Omega} h = -\frac{3}{2}\alpha l - 6\alpha m + \frac{3}{2}\alpha\sigma \ , \tag{16}$$

$$\xi = \beta(\sigma + m) + (1-\beta)(4m + h) \ , \qquad (17)$$

$$l = \frac{1}{\omega t_{\rm ps}+1}\xi - (\Omega t_{\rm ps})\frac{\partial {\rm ln}\Pi_0}{\partial {\rm ln} r}\frac{1}{\omega t_{\rm ps}+1}u \ , \qquad (18)$$

where κ is the epicyclic frequency defined as $\kappa^2 \equiv 2\Omega(2\Omega + rd\Omega/dr)$.

Before numerical calculations, we would point out that, for long-wavelength unstable modes, the second term on the right hand side of Eq. (18) is significantly less than the first term, thus the equation can be reduced to

$$l = \frac{1}{\omega t_{\rm ps}+1}\xi \ . \qquad (19)$$

The reason for the above simplification is as follows. Substituting equation (14) into (18), we will have

$$\left[\frac{\kappa^2}{2\Omega^2}\frac{(r\Omega)^2\Sigma_0}{i\alpha k r \Pi_0} + (\Omega t_{\rm ps})\frac{\partial {\rm ln}\Pi_0}{\partial {\rm ln} r}\frac{1}{\omega t_{\rm ps}+1}\right] u = \frac{1}{\omega t_{\rm ps}+1}\xi, (20)$$

For standard thin discs, $\partial{\rm ln}\Pi_0/\partial{\rm ln}r$ and $\kappa^2/(2\Omega^2)$ are around unity. Thus, for long-wavelength unstable modes, on the left hand side of Eq. (20), the ratio of the second term to the first term is

$$\left|\left[(\Omega t_{\rm ps})\frac{\partial {\rm ln}\Pi_0}{\partial {\rm ln} r}\frac{1}{\omega t_{\rm ps}+1}\right] \Big/ \left[\frac{\kappa^2}{2\Omega^2}\frac{(r\Omega)^2\Sigma_0}{i\alpha k r \Pi_0}\right]\right|$$

$$\approx \left|\frac{\partial {\rm ln}\Pi_0}{\partial {\rm ln} r}\right| \left|\frac{1}{\omega t_{\rm ps}+1}\frac{1}{\kappa^2/(2\Omega^2)}\right| \left|2\frac{t_{\rm ps}}{t_{\rm th}}\frac{H}{r}\right| |kH| \ll 1 \ . \qquad (21)$$

Thus, equation (20) can be simplified as

$$\left[\frac{\kappa^2}{2\Omega^2}\frac{(r\Omega)^2\Sigma_0}{i\alpha k r \Pi_0}\right] u = \frac{1}{\omega t_{\rm ps}+1}\xi \ ,$$

which is equivalent to Eq. (19).

For non-trivial solutions of σ, ξ, u, h, m, and l, we obtain the following dispersion relation from equations (13)-(17) and (19),

$$c_1(\frac{\omega}{\Omega})^3 + c_2(\frac{\omega}{\Omega})^2 + c_3(\frac{\omega}{\Omega}) + c_4 = 0 \ , \qquad (22)$$

where

$$c_1 = (\Omega t_{\rm ps})\left(\frac{7-6\beta}{2} + \frac{\beta}{\gamma-1} - \frac{7}{2}\beta\frac{4-3\gamma}{\gamma-1}\frac{1-\beta}{4-3\beta}\right) \ ,$$

$$c_2 = \left(\frac{7-6\beta}{2} + \frac{\beta}{\gamma-1} - \frac{7}{2}\beta\frac{4-3\gamma}{\gamma-1}\frac{1-\beta}{4-3\beta}\right) + \frac{3\alpha(1+\beta)}{(4-3\beta)}(\Omega t_{\rm ps}) \ ,$$

$$c_3 = 2\alpha(kH)^2\left(\frac{\Omega}{\kappa}\right)^2\left(\frac{9-6\beta}{2} + \frac{\beta}{\gamma-1} - \frac{9}{2}\beta\frac{4-3\gamma}{\gamma-1}\frac{1-\beta}{4-3\beta}\right) - \frac{3\alpha}{2} + \frac{3\alpha(1+\beta)}{(4-3\beta)} \ ,$$

$$c_4 = 3\alpha^2(kH)^2\left(\frac{\Omega}{\kappa}\right)^2\frac{2+3\beta}{4-3\beta} \ .$$

When $t_{\rm ps} \to 0$, the above dispersion relation is reduced to the form in the α stress scenario (e.g., Kato et al. 2008, p. 180).

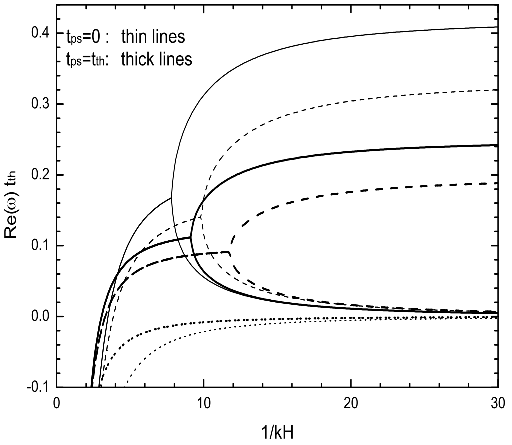

Figure 1. Variation of the growth rate with the radial wavelength of perturbation. The thin and thick lines correspond to the standard α stress prescription and the stress evolution process with $t_{\rm ps} = t_{\rm th}$, respectively. The solid, dashed, and dotted lines correspond to $\beta = 0.01$, 0.1, and 0.4, respectively.

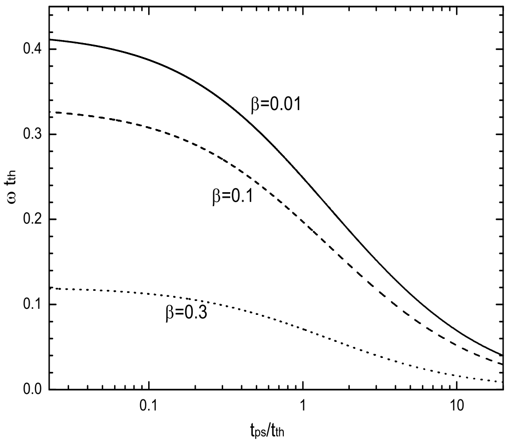

Figure 2. Variation of the growth rate with the timescale of stress delay in the long-wavelength limit ($kH \to 0$).

We numerically solve the dispersion equation (22) to obtain the growth rates of unstable modes. In our calculation, we fix $\alpha = 0.1$ and $\gamma = 5/3$. There exist three modes for each given radial wavelength of perturbations. Among the three modes, one is always stable corresponding to a negative ω, and is therefore neglected in the following analysis. We study the dispersion relation for two cases: (i) with stress evolution process ($t_{\rm ps} = t_{\rm th}$); (ii) with the standard α stress ($t_{\rm ps} = 0$). The growth rates of the remaining two modes are shown in Figure 1. In this figure, the thick and thin lines correspond to the stress evolution process and the α stress prescription, respectively. The solid, dashed, and dotted lines represent the solutions with $\beta = 0.01$, 0.1, and 0.4, respectively, where $\beta = 0.4$ is the well known critical value for the thermal stability with the α prescription. It is shown that the growth rate of thermally unstable modes (the upper branch) in the stress evolution scenario is significantly smaller than that in the α stress case. On the contrary, the growth rates of the viscously unstable modes (the lower branch) of the above two cases are similar. Here, the thermal timescale $t_{\rm th}$ is calculated by

$$t_{\rm th} = \frac{E}{Q_{\rm vis}^{+}} = \frac{2[3(1-\beta)(\gamma-1)-\beta]}{3(\gamma-1)} \frac{1}{\alpha\Omega} \ . \tag{23}$$

Figure 1 indicates that, even though the stress evolution process does not change the stability criterion, it may have significant influence on the growth rate of the thermally unstable mode.

For further investigation, we calculate the solutions under the long-wavelength limit, i.e., $kH \to 0$. In such case, the non-zero roots of the dispersion equation (22) are,

$$\omega = \frac{1}{2At_{\rm th}} \left[-(\frac{At_{\rm th}}{t_{\rm ps}}+1) \pm \sqrt{(\frac{At_{\rm th}}{t_{\rm ps}}+1)^2 + 2\frac{At_{\rm th}}{t_{\rm ps}}\frac{2-5\beta}{1+\beta}} \right] , \tag{24}$$

where

$$A = \frac{\left(\frac{7-6\beta}{2} + \frac{\beta}{\gamma-1} - \frac{7}{2}\beta\frac{4-3\gamma}{\gamma-1}\frac{1-\beta}{4-3\beta}\right)}{[3(1-\beta)+\frac{\beta}{\gamma-1}]} \frac{4-3\beta}{2(1+\beta)} \ .$$

The above equation shows the relationship between the growth rate ω and the timescale of stress delay $t_{\rm ps}$.

For the case of $t_{\rm ps}/t_{\rm th} \gg 1$, Eq. (24) is simplified as

$$\omega = \frac{1}{2t_{\rm ps}} \frac{2-5\beta}{1+\beta} \sim \frac{1}{t_{\rm ps}} \ , \tag{25}$$

which means that if $t_{\rm ps}$ is sufficiently larger than $t_{\rm th}$, the growing timescale of thermal instability is around $t_{\rm ps}$. On the contrary, for the case of $t_{\rm ps}/t_{\rm th} \ll 1$, Eq. (24) is reduced to

$$\omega = \frac{1}{2At_{\rm th}} \frac{2-5\beta}{1+\beta} \sim \frac{1}{t_{\rm th}} \ . \tag{26}$$

The above growth rate is exactly the same as that in the α stress case, in which the growing timescale of thermal instability is around $t_{\rm th}$.

Figure 2 shows the variation of the growth rate of the thermally unstable mode in the long-wavelength limit with $t_{\rm ps}$ for $\beta = 0.01$, 0.1, and 0.3. The figure clearly illustrates that, for the case of $t_{\rm ps} \gtrsim t_{\rm th}$, the stress evolution process will have essential effects on the thermal instability since the growth rate is significantly decreased.

5 CONCLUSIONS AND DISCUSSION

In this paper, the stress evolution process, which was ignored in previous works, is taken into account in the linear stability analysis of standard thin accretion discs. We show the variation of the growth rate of thermally unstable modes with the wavelength of perturbations for two cases: with and without stress delay. We find that the growth rate with stress delay can be apparently lower than that without stress delay. We also make some analytical approximation for the growth rate in long-wavelength limit, and present the relationship between the specific growth rate and the timescale of stress delay. In conclusion, the stress evolution process may have essential influence on the thermal instability by significantly decreasing the growth rate, in particular for the case in which the timescale of stress delay is comparable to or even larger than the thermal timescale.

In a real system the timescale of stress delay remains unclear. We would argue that this timescale is possibly comparable to the thermal timescale as follows. In simulations with an initially weak toroidal or poloidal magnetic field, the magnetic energy may first experience an exponential growth during the first few orbits due to the linear instability, and then will be followed by the nonlinear evolution. Finally, a saturated quasi-steady state phase may form. Totally, it will take $15 \sim 20$ orbits for the system to enter a fully turbulent state (e.g., Hawley et al. 1996; Fromang & Papaloizou 2007). This implies that the evolution timescale of the magnetoturbulence is around $15 \sim 20$ times of the dynamical timescale $t_{\rm dyn}$, which can be regarded as a duration around the thermal timescale $t_{\rm th}$ (e.g., $t_{\rm th} \sim t_{\rm dyn}/\alpha$ and $\alpha = 0.1$).

As mentioned in the first section, when the theory of the limit cycle behaviour between the standard thin disc and the slim disc is applied to the observational quasi-periodic variability of GRS 1915, there exists some conflict between the theory and the observation on the duration ratio $t_{\rm high}/t_{\rm low}$ and the luminosity ratio $L_{\rm high}/L_{\rm low}$. In our opinion, the stress evolution process may improve the theory to explain observations due to the following reasons. When the flow suffers thermal instability, the growth rate of $\dot{M}$ can be significantly decreased by the stress delay. We therefore can expect a relatively lower $\dot{M}$ for the outburst phase, thus a corresponding lower $L_{\rm high}/L_{\rm low}$. As a consequence, for a certain fixed mass accretion rate supply at outer boundary, if $\dot{M}$ at outburst phase drops, the duration of this phase will therefore become longer, thus a moderate value of $t_{\rm high}/t_{\rm low}$ should appear. In other words, the influence of the stress delay on the growth rate may result in moderate ratios of duration and luminosity of the outburst phase to the quiescent one, which will be more likely to explain the observational results than previous calculations. The further investigation on this issue may require time-dependent numerical calculations including the stress evolution process.

Moreover, we would point out the possible application of the stress evolution process to another geometrically thin disc, namely the Shapiro-Lightman-Eardley disc (the SLE disc, Shapiro et al. 1976), which was originally introduced as the inner region of a thin disc to provide hard X-ray emission. However, it is known that the SLE disc is viscously stable but suffers thermal instability. If the stress evolution process is taken into consideration in the SLE model, and the timescale of stress delay is comparable to the thermal timescale, we can therefore expect the existence of a quasi-stable SLE disc since the decreased growth rate of thermal instability may not completely destroy the disc and the viscous stability may help to suppress the thermal instability in the viscous timescale.

ACKNOWLEDGMENTS

We thank Shoji Kato and Sheng-Ming Zheng for beneficial discussion. This work was supported by the National Basic Research Program of China under grant 2009CB824800, and the National Natural Science Foundation of China under grants 10833002 and 11073015.

REFERENCES

Abramowicz, M. A., Czerny, B., Lasota, J. P., Szuszkiewicz, E. 1988, ApJ, 332, 646

Balbus S. A., Papaloizou J. C. B., 1999, ApJ, 521, 650

Belloni T., Méndez M., King A. R., van der Klis M., van Paradijs J., 1997, ApJ, 479, L145

Czerny, B., Siemiginowska, A., Janiuk, A., Nikiel-Wroczyński, B., Stawarz, L, 2009, ApJ, 698, 840

Fromang, S., Papaloizou, J. 2007, A&A, 476, 1113

Gierliński, M. Done, C. 2004, MNRAS, 347, 885

Hawley, J. F., Gammie, C. F., Balbus, S. A. 1996, ApJ, 464, 690

Hirose, S., Krolik, J. H., Blaes, O. 2009, ApJ, 691, 16

Janiuk, A., Czerny, B., Siemiginowska, A. 2002, ApJ, 576, 908

Kato, S., Fukue, J., Mineshige, S. 2008, Black-Hole Accretion Disks: Towards a New Paradigm (Kyoto: Kyoto Univ. Press)

Lightman, A., Eardley, D. 1974, ApJ, 187, L1

Li, S.-L., Xue, L., Lu, J.-F. 2007, ApJ, 666, 368

Nayakshin, S., Rappaport, S., Melia, F. 2000, ApJ, 535, 798

Shakura, N. I., Sunyaev, R. A. 1973, A&A, 24, 337

Shapiro, S. L., Lightman, A. P., Eardley, D. M. 1976, ApJ, 204, 187

Szuszkiewicz, E., Miller, J. C., 2001, MNRAS, 328, 36

Wu, Q.-W. 2009, ApJ, 701, L95

Wu, Y. X., Yu, W., Li, T. P., Maccarone, T. J., Li, X. D. 2010, ApJ, 718, 620

This paper has been typeset from a TEX/ LATEX file prepared by the author.